

UC Berkeley

UC Berkeley Previously Published Works

Title

3D simulation of tsunami wave induced by rock slope failure using coupled DDA-SPH

Permalink

<https://escholarship.org/uc/item/9v49c839>

ISBN

9781634395236

Authors

Mikola, RG

Sitar, N

Cahill, EG

et al.

Publication Date

2014

Peer reviewed

3D Simulation of Tsunami Wave Induced by Rock Slope Failure Using Coupled DDA-SPH

Roozbeh Geraili Mikola,

Jacobs Associates, San Francisco, CA, USA

Nicholas Sitar,

Edward G. Cahill and John R. Cahill Professor, Dept. of Civil and Environmental Engineering, UC Berkeley, Berkeley, CA, USA

Copyright 2014 ARMA, American Rock Mechanics Association

This paper was prepared for presentation at the 48th US Rock Mechanics / Geomechanics Symposium held in Minneapolis, MN, USA, 1-4 June 2014.

This paper was selected for presentation at the symposium by an ARMA Technical Program Committee based on a technical and critical review of the paper by a minimum of two technical reviewers. The material, as presented, does not necessarily reflect any position of ARMA, its officers, or members. Electronic reproduction, distribution, or storage of any part of this paper for commercial purposes without the written consent of ARMA is prohibited. Permission to reproduce in print is restricted to an abstract of not more than 200 words; illustrations may not be copied. The abstract must contain conspicuous acknowledgement of where and by whom the paper was presented.

ABSTRACT: We present a three dimensional fluid-structure coupling between SPH and 3D-DDA for modelling rock-fluid interactions. The Navier-Stokes equation is simulated using the SPH method and the motions of the blocks are tracked by a Lagrangian algorithm based on a newly developed, explicit, 3D-DDA formulation. The coupled model is employed to investigate the water entry of a sliding block and the resulting wave(s). The coupled SPH-DDA algorithm provides a promising computational tool to for modelling a variety of solid-fluid interaction problems in many potential applications in hydraulics, rock mass stability, and in coastal and offshore engineering.

1. INTRODUCTION

Landslides, rock falls, and debris avalanches can generate significant tsunami waves in the coastal areas. Although landslide-generated tsunamis are decidedly more localized than seismically generated tsunamis, they can produce destructive coastal run-up and cause severe damage, especially where the wave energy is trapped by the confines of inlets or semi-enclosed embayments [1, 2]. Among the best known examples of catastrophic landslide-generated tsunamis are the 1958 Lituya Bay, the 1963 Vaiont Valley, and the 1934 Tafjord events. The Lituya Bay event of July 10, 1958 was caused by a large rockslide at the head of Lituya Bay, Southeast Alaska, that produced a giant wave that impacted the sides of the inlet to a height of 525 m [1, 3, 4]. The Vaiont Valley event occurred on October 9, 1963 when a massive rock slide fell 175 m into a reservoir in the Vaiont Valley, North Italy, creating a wave that destroyed a town and killed approximately 3000 people [1, 5]. In 1934 roughly $1.5 \cdot 10^6$ m³ of rock plunged into the Tafjord in Western Norway [6]. fjord and produced

water run-up heights up to 60 m which resulted in the death of 41 people.

The complexity of the water-rock mass interaction has been studied using both experimental and analytical methods. Fritz [7] and Fritz et al. [8, 9, and 10] performed experiments to study waves created by a deformable landslide in a 2D wave tank. Zweifel et al. [11] also used experiments to study the non-linearity of impulse waves. Huber and Hager [12] looked at both 3D and 2D impulse waves. Raichlen and Synolakis [13] performed experiments with a freely sliding wedge representing a land slide. Liu et al. [14] used the same type of experiments to validate a numerical model, based on the large-eddy-simulation approach. Recently, Saelevik et al. [6] performed two-dimensional experiments of wave generation from the possible Akneset rock slide using solid block modules in a transect with a geometric scaling factor of 1:500.

The numerical simulation approaches used a number of different methods. For example, Harbitz [15] simulated tsunamis generated by Storegga slides using linear shallow water equations. Jiang and Leblond [2, 16], Fine et al. [17], Thomson et al. [18], Imamura et al.

[19], Titov and Gonzalez [20] used nonlinear shallow water approximation to model the slide-water system as a two-layer flow. Lynett and Liu [21] discussed the limitations of the depth-integrated models with regards to landslide-generated waves, and developed fully nonlinear weakly dispersive model for submarine slides that is capable of simulating waves from relatively deep water to shallow water. Grilli and Watts [22] derived and validated a two-dimensional fully nonlinear dispersive model that does not have any restrictions on the wave amplitude, wavelength, or landslide depth, and describes the motion of the landslide by the position of its center of mass.

The limitation of these approaches has been the assumption that the slide mass, soil or rock, could be approximated as an equivalent fluid mass or a continuous solid. While this approximation may be adequate and valid in many instances, it is desirable to be able to model the complexity of individual rock blocks interacting with water independently, thus allowing a greater flexibility in the type of phenomena that is modelled.

In this paper we present Discontinuous Deformation Analysis (DDA) coupled with Smoothed Particles Hydrodynamics (SPH) numerical model for the study of rock-fluid interaction in 3-D. Since its introduction by Shi [23], 2-D DDA has been extensively developed in theory and computer codes, and there has been a significant interest in extending the formulation to 3-D. Shi [24, 25] presented the 3-D block matrices such as mass matrix, stiffness matrix, point load matrix, body load matrix, initial stress matrix and fixed point matrix. Grayeli and Hatami [26] presented formulation of coupled DDA and FEM in three dimensions. Mikola and Sitar [27] presented a new explicit time integration procedure for the solution of 3D-DDA algorithm in order to reduce the computational effort and memory requirement. They utilized a uniform spatial discretization method to eliminate unnecessary contact computations and the contact resolution was handled by FCP approach [28], HalfEdge data structure was used to handle the frequent navigation into the topological information associated with polyhedral blocks.

Smoothed Particle Hydrodynamics (SPH), a meshless Lagrangian method, is a method that can capture the complexity of free surface flow with fragmentation and splashes. The SPH technique was conceived by Lucy [29] and further developed by Gingold and Monaghan [30] for treating astrophysical problems. Its main advantage is the absence of a computational grid or mesh, since it is a Lagrangian particle based method. This allows the possibility of easily modelling flows with a complex geometry or flows where large deformations or the appearance of a free surface occur.

Our interaction model uses SPH to model the fluid and the rigid body solids are modelled using 3-D DDA [31]. However, the general interaction model we propose works with any type of solid model representation as long as the object is represented by a polygonal surface and the fluid by Lagrangian particles.

2. EXPLICIT TIME INTEGRATION SCHEME

DDA models a discontinuous material as a system of individually deformable blocks that move independently without interpenetration. Following the second law of thermodynamics, a mechanical system under loading must move or deform in a direction that produces the minimum total energy of the whole system. For a block system the total energy consists of the kinetic energy, potential energy, strain energy and the dissipated energy. In DDA individual blocks form a system of blocks through contacts among blocks and displacement constrains on a single block. For a system of n blocks the simultaneous equilibrium equations, derived by minimizing the total energy Π of the block system.

Let D_n and D_{n+1} denote the approximation to the values $D(t)$ and $D(t+1)$ for a time step Δt , respectively. Recall the system of equations Eq. 1 of motion for a DDA system [23]:

$$M\ddot{D}_{n+1} + C\dot{D}_{n+1} + KD_{n+1} = F_{n+1} \quad (1)$$

with $D(0) = 0, \dot{D}(0) = \dot{D}_0$ as initial boundary conditions. In the above M, C, K are the global mass, damping and stiffness matrices, F is the time dependent applied force vector, and \ddot{D}, \dot{D}, D and denote acceleration, velocity and displacement vectors, respectively.

Original DDA time integration scheme adopts the Newmark [32] approach, which for a single degree of freedom can be written in the following manner:

$$u_{i+1} = u_i + \Delta t \dot{u}_i + \left(\frac{1}{2} - \beta\right) \Delta t^2 \ddot{u}_i + \beta \Delta t^2 \ddot{u}_{i+1} \quad (2)$$

$$\dot{u}_{i+1} = \dot{u}_i + (1 - \gamma) \Delta t \ddot{u}_i + \gamma \Delta t \ddot{u}_{i+1} \quad (3)$$

Where \ddot{u}, \dot{u} , and u are acceleration, velocity, and displacement respectively, Δt is the time step, β and γ are the collocation parameters defining the variation of acceleration over the time step. Unconditional stability of the scheme is assured for $2\beta \geq \gamma \geq 0.5$. DDA integration scheme uses $\beta = 0.5$ and $\gamma = 1$, thus setting the acceleration at the end of the time step to be constant over the time step. This approach is implicit and unconditionally stable. Substituting Eqs. 2 and 3 into Eq. 1 results in the system of equations for solving the dynamic problem:

$$\left(\frac{2}{\Delta t^2} M + \frac{2}{\Delta t} C + K\right) D_{n+1} = F_{n+1} + \left(\frac{2}{\Delta t} M + C\right) \dot{D}_n \quad (4)$$

The solution of Eq. 4 requires assembling the global mass and stiffness matrices and solving the coupled system of equations using a direct matrix inverse operation or an iterative solver. The global stiffness matrix, K , includes the sub-matrix representing deformability of blocks and contacts, with contact matrices as off-diagonal terms.

Shi [23] solved the global equations iteratively by repeatedly adding and removing contact springs (penalty values) until each of the contacts converges to a constant state at each time step. This procedure of adding and removing contact springs (penalty values) is known as open-close iterations in the DDA literature [33]. If contact convergence is not achieved typically within six iterations, the time step is reduced and the analysis is repeated with the reduced time step. The incremental displacement is restricted also by user-specified displacement limit to enforce infinitesimal displacements. If the incremental displacement is greater than the threshold, Δt is divided by three and the analysis is repeated. Large values of Δt may cause large penetrations at contact points; which results in more iterations to satisfy the penetration threshold. Also, large penetrations result in large contact matrices which can reduce the diagonal dominance of the global stiffness matrix leading to poorly conditioned system of equations.

In the explicit solution procedure presented herein the discrete blocks are integrated explicitly by the central difference method, which gives

$$u_{i+1} = u_i + \Delta t_{i+1} \dot{u}_i \quad (5)$$

$$\dot{u}_{i+1/2} = \dot{u}_{i-1/2} + \frac{1}{2}(\Delta t_{i+1} + \Delta t_i) \ddot{u}_i \quad (6)$$

Where $i, i+1/2$ and $i-1/2$ refer to the increment number and mid-increment numbers

$$\ddot{u}_i = M^{-1}(F_i - I_i) \quad (7)$$

where M is mass matrix, F the applied load vector and I is the internal force vector. The equations relating these values to each other are solved locally for each time-step. Moreover, since there is no need to solve a complete system of equations, the incremental calculations for each degree of freedom are done independently at the local level. This uncoupling of the equations of motion is one of the major advantages of explicit integration schemes. In contrast to the implicit time integration scheme, the explicit solution scheme eliminates the need for assembly of global mass or stiffness matrices and inversion of the global matrix. However, computations are conditionally stable, i.e., the time-step size must be smaller than a certain critical value (critical time step, Δt_c) for numerical errors not to grow unbounded. The time increments must satisfy the well-known criterion

$$\Delta t \leq \frac{2}{\omega_{\max}} \quad (8)$$

where ω_{\max} is the element maximum eigenvalue.

3. NUMERICAL MODELING OF WATER FLOW

3.1. Navier-Stokes Equations.

The dynamic behaviour of a viscous fluid, like water, is completely described by the so-called Navier-Stokes equations (NSEs). The equations for incompressible fluids are the mass conservation equation and the momentum conservation equation. Many forms of the NSEs appear in the literature. Equations (9) and (10) represent a simplified version for incompressible fluids.

$$\nabla \cdot u = 0 \quad (9)$$

$$\frac{\delta u}{\delta t} + (u \cdot \nabla)u = -\frac{1}{\rho} \nabla p + \nu \nabla^2 u + f \quad (10)$$

where ρ , u , P , ν , g are density, velocity, pressure, dynamic viscosity coefficient of the fluid and gravitational acceleration, respectively. The first equation is the incompressibility condition. The second equation is called momentum equation which describes how fluid moves due to the forces.

3.2. Smoothed Particle Hydrodynamics (SPH) equations

The SPH is an interpolation method for fluid motion simulation. SPH uses field quantities defined only at discrete particle locations and can be evaluated anywhere in space. SPH distributes quantities in a local neighborhood of the discrete locations using radial symmetrical smoothing kernels. A scalar value A is interpolated at location r by a weighted sum of contributions from the particles. In SPH, a physical value at position x is calculated as a weighted sum of physical values φ_j of neighbouring particles j

$$A_s(X) = \sum_j m_j \frac{\varphi_j}{\rho_j} W(X - X_j) \quad (11)$$

where m_j , ρ_j , X_j are the mass, density and position of particle j , respectively and W is a weight function.

The use of particles instead of a stationary grid simplifies these two equations substantially. First, because the number of particles is constant and each particle has a constant mass, mass conservation is guaranteed and (9) can be omitted completely. Second, the expression $\frac{\delta u}{\delta t} + (u \cdot \nabla)u$ on the left hand side of (10) can be replaced by the substantial derivative $\frac{\delta u}{\delta t}$. Since the particles move with the fluid, the substantial derivative of the velocity field is simply the time derivative of the velocity of the particles meaning that the convective term $u \cdot \nabla \cdot u$ is not needed for particle systems. We regard

NSEs as the governing equations, and calculate density, pressure and viscosity force separately using SPH numerical methods. The density of fluid is calculated with (12) as

$$\rho_j = \sum_j m_j W(r_i - r_j, h) \quad (12)$$

Accuracy of the algorithm highly depends on the smoothing kernels. For our implementation we used the following kernel:

$$W(r, h) = \frac{315}{64\pi h^9} \begin{cases} (h^2 - r^2)^3 & (0 \leq r \leq h) \\ 0 & (r > h) \end{cases} \quad (13)$$

We use the weight functions proposed by Muller et al. [34] and a modified solution is obtained for pressure force guaranteeing the symmetry of forces:

$$f_i^{pressure} = -\sum_j m_j \frac{p_i - p_j}{2\rho_j} \nabla W_{spiky}(r_i - r_j, h) \quad (14)$$

For pressure computations we use Debrun's spiky kernel [34]:

$$\nabla W_{spiky}(r, h) = \frac{45}{\pi h^6} \begin{cases} \left(\frac{h^2 + r^2}{r} - 2h \right) r & (0 \leq r \leq h, r = |r|) \\ 0 & (r > h) \end{cases} \quad (15)$$

The pressure at particle locations has to be calculated first, which can be computed via the ideal gas equation:

$$p = kr \quad (16)$$

where k is a gas constant that depends on the temperature. A modified version - which we used in our implementation - makes the simulation numerically more stable:

$$p = k(\rho - \rho_0) \quad (17)$$

where ρ_0 is the at-rest density. Applying the SPH rule to the viscosity term also yields to asymmetric forces because the velocity field varies. A symmetric expression is obtained using velocity differences:

$$f_i^{viscosity} = \mu \sum_j m_j \frac{v_i - v_j}{\rho_j} \nabla^2 W_{viscosity}(r_i - r_j, h) \quad (18)$$

Muller et al. [34], designed a kernel for the computation of viscosity forces as follows:

$$\nabla^2 W_{viscosity}(r, h) = \frac{45}{\pi h^6} \begin{cases} (h - r) & (0 \leq r \leq h, r = |r|) \\ 0 & (r > h) \end{cases} \quad (19)$$

Finally, for the acceleration a_i of a particle i we have

$$a_i = \frac{1}{\rho_i} (f_i^{pressure} + f_i^{viscosity} + f_i^{external}) \quad (20)$$

where $f_i^{external}$ are external body forces such as gravity forces. We then use a simple Euler integrator in our simulations, which is first order accurate in position and velocity, and can be written as,

$$v_i(t + \Delta t) = v_i(t) + \Delta t a_i(t)$$

$$x_i(t + \Delta t) = x_i(t) + \Delta t v_i(t + \Delta t) \quad (21)$$

where Δt is the time step.

4. COUPLING BETWEEN SPH AND DDA

The coupling algorithm used here is parallel; fluid (SPH) and solid block (DDA) evolutions are calculated explicitly at the same time. In order to couple the SPH and DDA the interaction force between fluid particles and solid blocks needs to be estimated. We choose to employ a fairly standardized "repulsion" force to prevent a particle from penetrating the boundaries. This method was chosen for the ease with which multiple types of boundaries can be implemented. The repulsion force is implemented for both "wall boundaries" as well as "solid blocks". The no-penetration condition states that the fluid cannot penetrate the boundary surface. To repel the fluid particles from the boundary we use a penalty-force method:

$$f_i^{boundary} = (K_S d - (v \cdot n) K_D) \cdot n \quad (22)$$

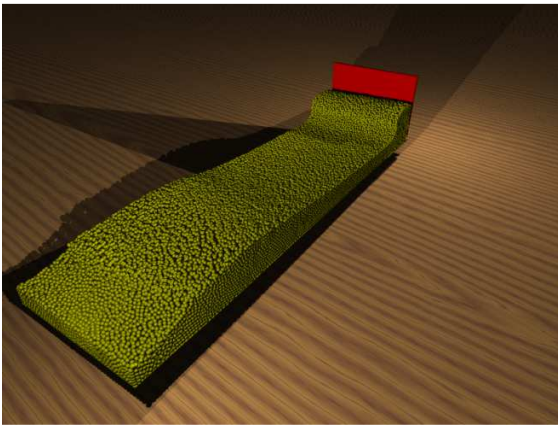
where K_S is the penalty force stiffness and K_D is the damping coefficient for the velocity v of an approaching fluid particle d is the penetrated distance measured normal to the boundary, and n is the unit-length surface normal. It can be seen from Equation (22) that the penalty force method behaves as a spring-based model, because the more a particle penetrates the boundary the more it is pushed away from the surface.

5. SIMULATIONS

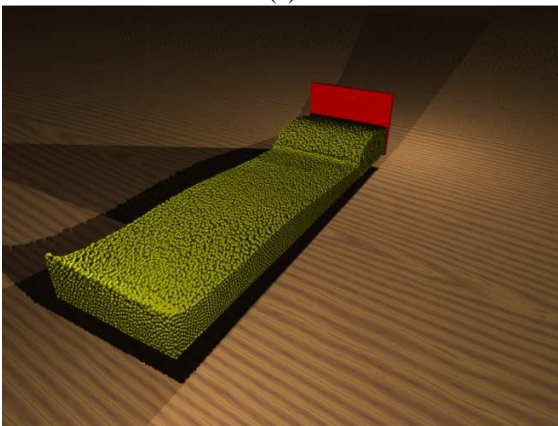
Three examples are presented to demonstrate the newly developed 3-D DDA algorithm. The scenes in the following examples have been rendered with POV-ray, a free code ray tracing rendering program [35].

5.1. Example 1- Wave Maker

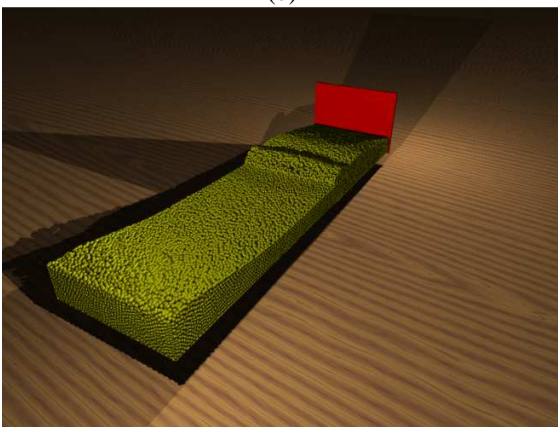
This simulation involves a wave maker in the form of an oscillating piston on the one end of the model, a straight line beach with a slope of 4% and a horizontal section 70 m long between the wave maker and the beach. The SPH simulation used almost 65000 particles and the boundaries as well as wavemaker itself have been simulated using as rigid blocks. Figure 1 shows the propagating waves onto the beach.



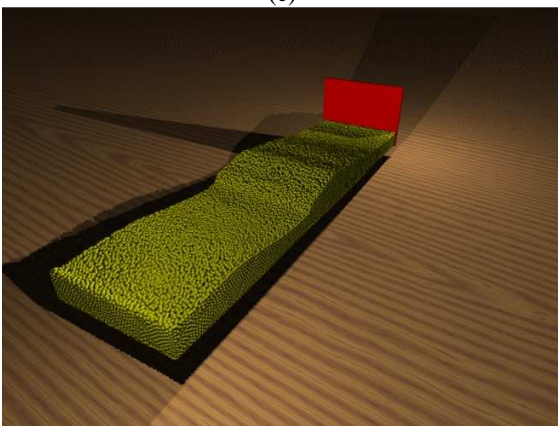
(a)



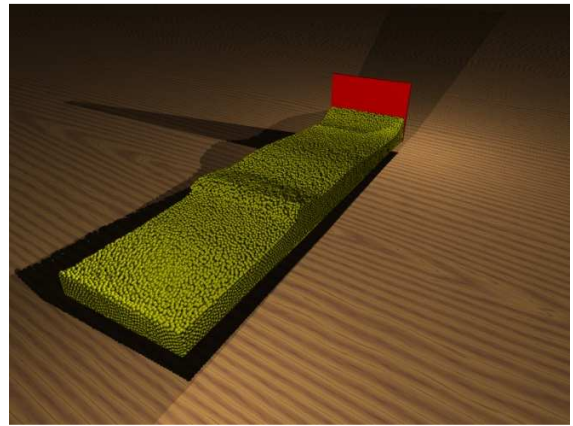
(b)



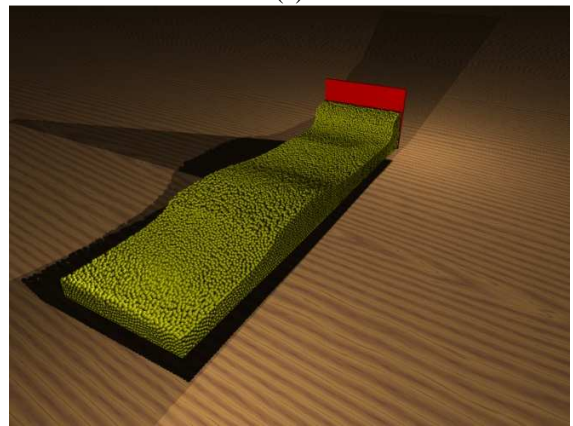
(c)



(d)



(e)

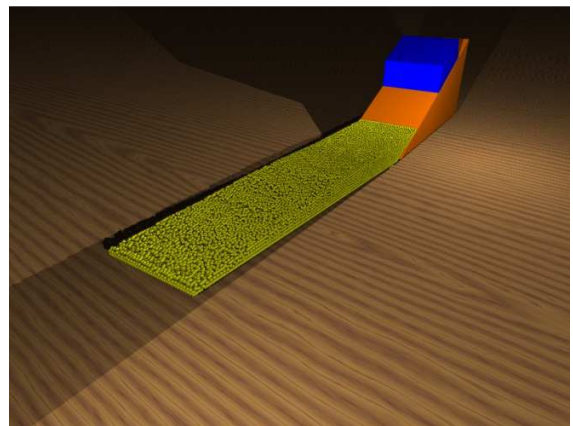


(f)

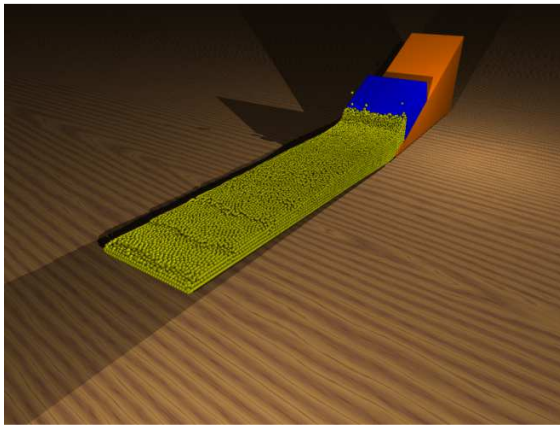
Figure 1. Particles and rigid block configuration for the wavemaker.

5.2. Example 2- Sliding Block

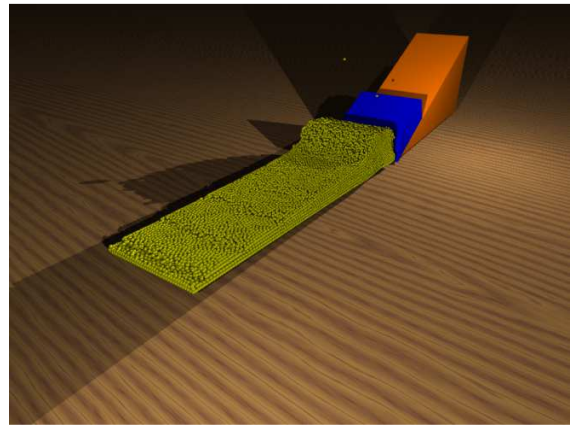
In this example we simulate waves generated by a rigid wedge sliding into water along an inclined plane. In this simulation water waves were generated by allowing a wedge shape block to freely slide down a plane inclined at 25° . The density of the wedge assumed to be 2500 kg/m^3 . The SPH simulation used almost 25000 particles and the boundaries as well as sliding block have been simulated as rigid blocks. Particles configuration due to sliding of the rigid wedge is presented at different times in Figure 2.



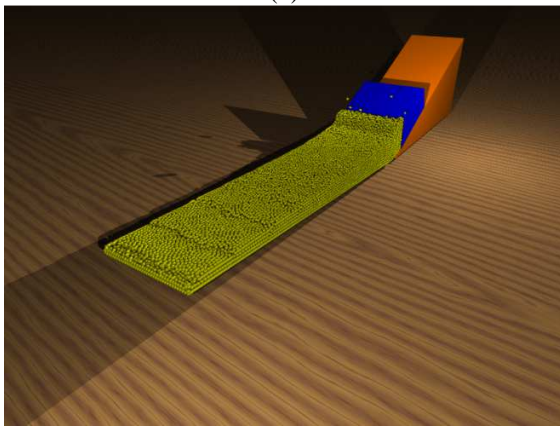
(a)



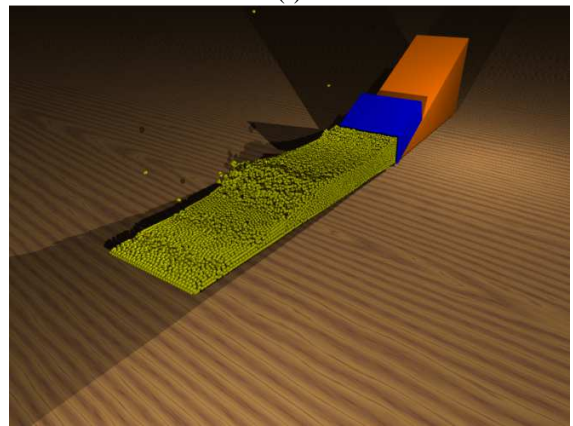
(b)



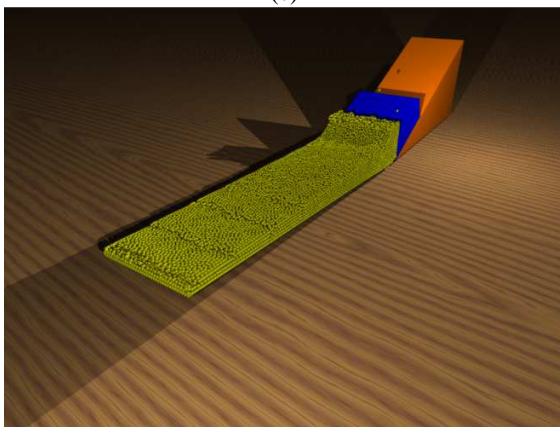
(f)



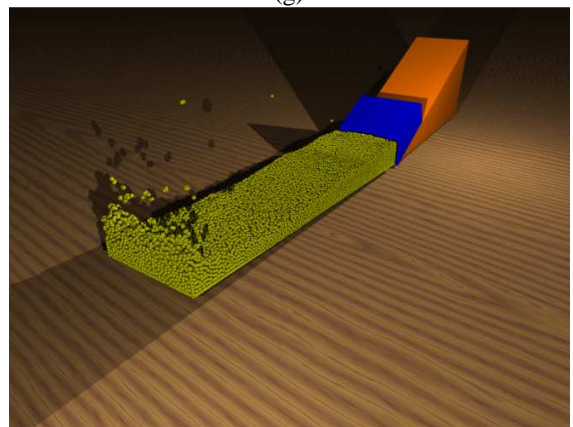
(c)



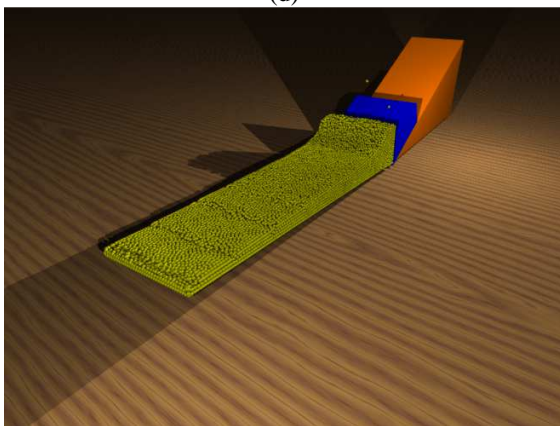
(g)



(d)



(h)

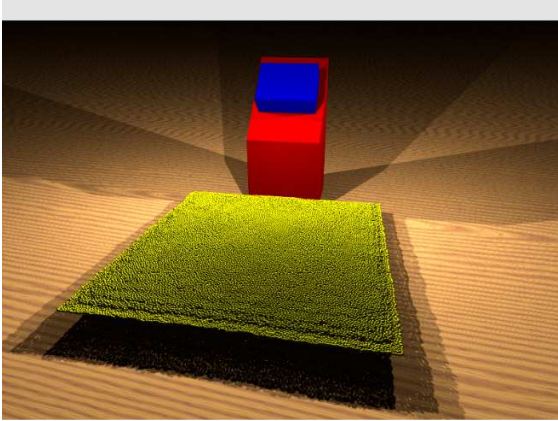


(e)

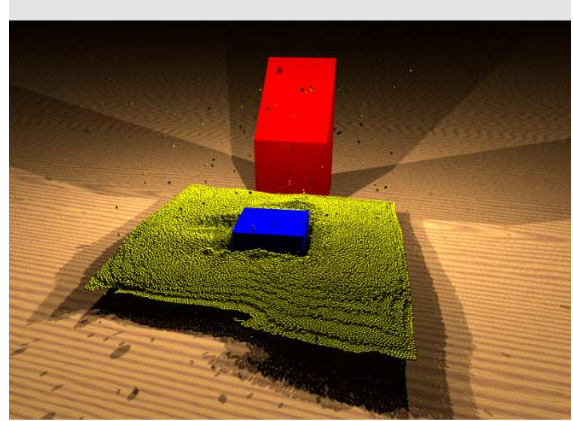
Figure 2. Particles and rigid blocks configuration for the rigid wedge sliding down a plane inclined 25° on the horizontal at different time steps.

5.3. Example 3- Impacting Block

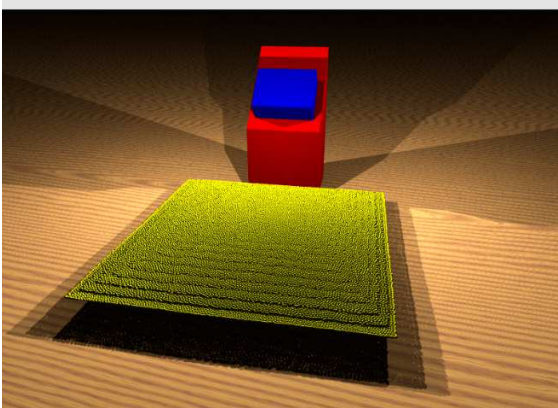
In this example we simulate waves generated by a rigid block impacting the water surface. In this simulation water waves were generated by allowing a block to freely slide down a plane inclined at 30° on the horizontal and impact the water surface. The density of the block assumed to be 2500 kg/m^3 . The SPH simulation used almost 100000 particles and the boundaries as well as sliding block have been simulated as rigid blocks. Particles configuration due to impact of the rigid block is presented at different times in Figure 3.



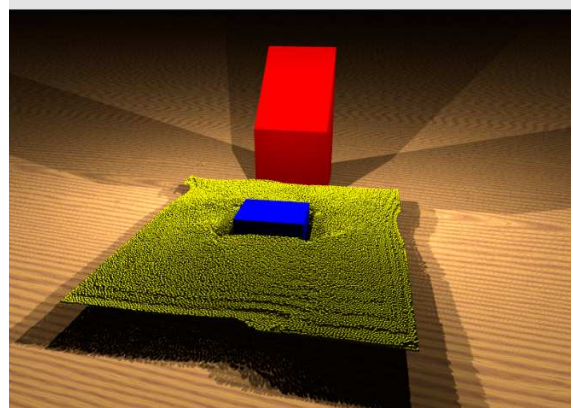
(a)



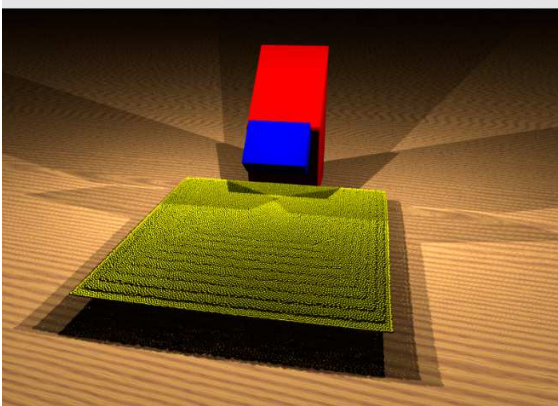
(e)



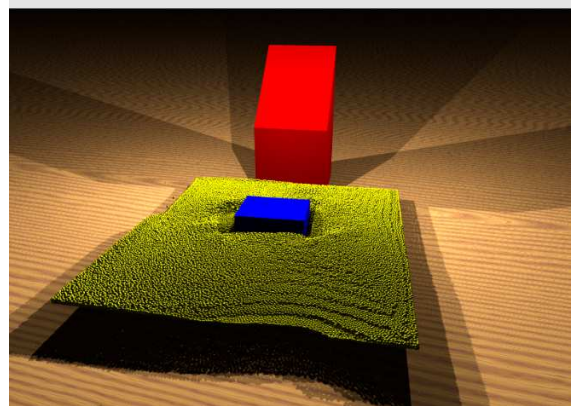
(b)



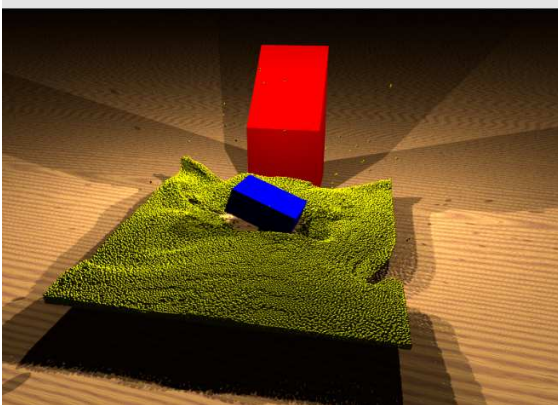
(f)



(c)



(g)



(d)

Figure 3. Particles and rigid blocks configuration for the rigid block impacting the water surface at different time steps.

6. SUMMARY

We present a highly efficient, three dimensional numerical model coupling the SPH method and 3D-DDA for modeling fluid-discrete solid body interaction problems. The explicit 3D-DDA formulation significantly simplifies and speeds up the computation which is essential for analysis of full scale problems. Similarly, the coupling algorithm is very efficient when dealing with fluid-structure interaction problems in the presence of a free-surface and is relatively simple to implement. The ability of SPH to fragment and

reconnect interfaces presents a great opportunity when modeling impacts of solids on fluids, and vice versa. The result of the example computations show that coupled SPH and DDA can be used to simulate dynamic fluid discrete block interactions in a variety of settings.

7. ACKNOWLEDGMENT

This research was supported in part by funding from the Edward G. Cahill and John R. Cahill Chair and Jacobs Associates generously provided the first author with the opportunity to pursue the research.

8. REFERENCES

1. Murty, T. S. (1977), Seismic Sea Waves – Tsunamis. Bull. Fish. Res. Board Canada 198, Ottawa, pp. 337.
2. Jiang, L. and Leblond, P. H. (1992), The Coupling of a Submarine Slide and the Surface Waves which it Generates, *J. Geophys. Res.* 97 (C8), 12,731–12,744.
3. Miller, D. J. (1960), The Alaska Earthquake on July 10, 1958: Giant Wave in Lituya Bay, *Bull. Seismoc. Soc. Am.* 50 (2), 253–266.
4. Lander, J. F. (1996), Tsunamis Affecting Alaska, 1737–1996 (Boulder, U. S. Dep. Comm., 1996), pp. 195.
5. Wiegel, R. L., Noda, E. K., Kuba, E. M., Gee, D. M., and Tornberg, G. F. (1970), Water Waves Generated by Landslides in Reservoirs, *J. Waterways, Harbors Coastal Eng., ASCE* 96, 307–333.
6. Saelevik, G. Jensen A., Pedersen G., Experimental investigation of impact generated tsunamis; related to a potential rock slide, Western Norway, Volume 56, Issue 9, September 2009, Pages 897–906.
7. Fritz, H.M., 2002. Initial phase of landslide generated impulse waves. PhD thesis, Swiss Federal Institute of Technology Zurich.
8. Fritz, H.M., Hager, W.H., Minor, H.E., 2003a. Landslide generated impulse waves. 1. instantaneous flow fields. *Experiments in Fluids* 35, 505–519.
9. Fritz, H.M., Hager, W.H., Minor, H.E., 2003b. Landslide generated impulse waves. 2. hydrodynamic impact craters. *Experiments in Fluids* 35, 520–532.
10. Fritz, H.M., Hager, W.H., Minor, H.E., 2004. Near field characteristics of landslide generated impulse waves. *Journal of Waterway, Port, Coastal and Ocean Engineering* 287–302.
11. Zweifel, A., Hager, W.H., Minor, H.E., 2006. Plane impulse waves in reservoirs. *Journal of Waterway, Port, Coastal and Ocean Engineering* 358–368.
12. Huber A, Hager WH (1997) Forecasting impulse waves in reservoirs, in Dix-neuvième Congrès des Grands Barrages, Florence, Commission Internationale des Grands Barrages, pp 993-1005
13. Raichlen, F., Synolakis, C., 2003. Runup from three dimensional sliding mass. *Long Waves Symposium*, Briggs, M., Koutitas. Ch. (Eds).
14. Liu J, Kong X, Lin G. 2004. Formulation of the three-dimensional discontinuous deformation analysis method. *Acta. Mech. Sinica.* 20(3):270–82. June.
15. Harbitz, C. B. (1992). "Model simulations of tsunamis generated by the Storegga slides." *Marine Geology*, 105, 1-21.
16. Jiang, L. and Leblond, P. 1994. Three-dimensional modeling of tsunami generation due to a submarine mudslide, *J. Phys. Oceanogr.* 24(3), 559–572.
17. Fine, I., Rabinovich, A., Kulikov, E., Thomson, R., and Bornhold, B. 1998. Numerical modelling of landslide-generated tsunamis with application to the Skagway Harbor tsunami of November 3, 1994. In *Proc. Int. Conf. on Tsunamis*, Paris, pp. 211–223.
18. Thomson, R.E., Rabinovich, A.B., Kulikov, E.A., Fine, 2001. I.V., and Bornhold, B.D., On numerical simulation of the landslide-generated tsunami of November 3, 1994 in Skagway Harbor, Alaska. In: *Tsunami Research at the End of a Critical Decade* (Hebenstreit, G.T., ed.), (Kluwer 2001), pp. 243–282.
19. Imamura, F., K.Hashi and MD. M.A.Imteaz; Modeling for tsunamis generated by landsliding and debris flow, *Tsunami Research at the End of a Critical Decade*, Ed. by G.T.Hebenstreit, Kluwer Academic Pub., pp.209-228, 2001.
20. Titov, V. and Gonzalez, F., 2001. Numerical study of the source of the July 17, 1998 PNG tsunami. In: *Tsunami Research at the End of a Critical Decade*, (Hebenstreit, G.T., ed.), (Kluwer 2001), pp. 197–207.
21. Lynett, P. and Liu, P.F. 2002. A numerical study of submarine landslide generated waves and runup, *Proc. Roy. Soc. London A* 458, 2885–2910.
22. Grilli, S. and Watts, P. 2005. Tsunami generation by submarine mass failure. I: Modeling, experimental validation, and sensitivity analysis, *J. Waterw. Port. Coast. Ocean. Eng.* 131(6), 283–297, DOI 10.1061/(ASCE)0733-950X(2005)131:6(283).
23. Shi GH. 1993. Block system modeling by discontinuous deformation analysis. Southampton UK and Boston USA: Computational Mechanics Publications.
24. Shi GH. 2001a. Three-dimensional discontinuous deformation analysis. In: Bicenic N, editor. *Proceedings of the forth international conference on analysis of discontinuous deformation (ICADD-4)*, Glasgow, Scotland, June 6–8, p. 1–21.
25. Shi GH. 2001b. Three-dimensional discontinuous deformation analysis. In: Ellsworth et al., editors. *Proceedings of the 38th US rock mechanics symposium*, Washington DC, July 7–10, p. 1421–8.
26. Grayeli R, Hatami K, 2008. Implementation of the finite element method in the three-dimensional

- discontinuous deformation analysis (3D-DDA), *International Journal for Numerical and Analytical Methods in Geomechanics*, 32:1883–1902.
27. Geraili Mikola, R, Sitar N., Explicit Three Dimensional Discontinuous Deformation Analysis for Blocky System, 47th US Rock Mechanics/Geomechanics Symposium, June 23-26, 2013 , San Francisco, CA.
 28. Nezami E, Hashash YMA, Zhao D, Ghaboussi J, 2004. A fast contact detection algorithm for 3-D discrete element method. *Comput. Geotech.* 31 (7):575–87.
 29. Lucy L. B. 1977 A numerical approach to the testing of the fission hypothesis *Astron. J.* 82 1013–24.
 30. Gingold R. A. and Monaghan J. J. 1977. Smoothed particle hydrodynamics: theory and application to non-spherical stars *Mon. Not. R. Astron. Soc.* 181 375–89.
 31. Geraili Mikola, R., Sitar N., Next generation discontinuous rock mass models: 3-D and rock-fluid interaction, *Frontiers of Discontinuous Numerical Methods and Practical Simulations in Engineering and Disaster Prevention – Chen, Ohnishi, Zheng & Sasaki (Eds) © 2013 Taylor & Francis Group, London, ISBN: 978-1-138-00110-7.*
 32. Newmark, NM. 1959. A Method of Computation for Structural Dynamics”, *ASCE Journal of the Engineering Mechanics Division*, Vol. 85 No. EM3.
 33. Doolin DM. and Sitar N. 2004. Time integration in discontinuous deformation analysis DDA. *ASCE Journal of Engineering Mechanics*, 130:249-258.
 34. Muller, M., Charypar, D., and Gross, M. 2003. Particle based fluid simulation for interactive applications. In *SCA '03: Proceedings of the 2003 ACM SIGGRAPH/Eurographics symposium on Computer animation*, Eurographics Association, Airela-Ville, Switzerland, Switzerland, 154–159.
 35. Persistence of Vision Pty. Ltd. 2004. Persistence of Vision Raytracer (Version 3.6), <http://www.povray.org/download/>